Production of excited atomic hydrogen and deuterium from H_2, HD and D_2 photodissociation

2011 J. Phys. B: At. Mol. Opt. Phys. 44 045201

(http://iopscience.iop.org/0953-4075/44/4/045201)

J. Phys. B: At. Mol. Opt. Phys. **44** (2011) 045201 (7pp) doi:10.1088/0953-4075/44/4/045201

Production of excited atomic hydrogen and deuterium from H_2, HD and D_2 photodissociation

J R Machacek[1,2], V M Andrianarijaona[3], J E Furst[4], A L D Kilcoyne[5], A L Landers[6], E T Litaker[1], K W McLaughlin[7] and T J Gay[1]

[1] Behlen Laboratory of Physics, University of Nebraska, Lincoln, NE 68588, USA
[2] Australian National University, Canberra, ACT 2601, Australia
[3] Department of Physics, Pacific Union College, Angwin, CA 94508, USA
[4] School of Mathematical and Physical Sciences, University of Newcastle-Ourimbah, NSW 2258, Australia
[5] Lawrence Berkeley National Laboratory, Berkeley, CA 94720, USA
[6] Allison Laboratory, Auburn University, Auburn, AL 36849-5311, USA
[7] Department of Physics and Engineering, Loras College, Dubuque, IA 52001, USA

E-mail: jma107@physics.anu.edu.au

Received 25 August 2010, in final form 16 December 2010
Published 28 January 2011
Online at stacks.iop.org/JPhysB/44/045201

Abstract
We have measured the production of Lyman α and Balmer α fluorescence from atomic H and D for the photodissociation of H_2, HD and D_2 by linearly-polarized photons with energies between 22 and 64 eV. We discuss systematic uncertainties associated with our data, and compare our results with previous experimental results and *ab initio* calculations of the dissociation process. We comment on the discrepancies.

(Some figures in this article are in colour only in the electronic version)

1. Introduction

When vacuum-ultraviolet (VUV) light dissociates H_2, fluorescence from excited H photofragments can result. Recent experiments done at BESSY [1], Trieste [2], KEK [3] and the Advanced Light Source (ALS) [4] have measured the production of Lyman α (Lyα, $n = 2 \rightarrow n = 1$, 122 nm) and Balmer α (Hα, $n = 3 \rightarrow n = 2$, 656 nm) fluorescence as a function of the energy of the incident VUV light. These excitation functions are characterized by a broad maximum from 30 to 60 eV with substructure corresponding to different channels for the production of excited photofragments.

Excited H atoms are produced via (1) singly-excited molecular states which dissociate, (2) direct 'non-resonant' production of excited H_2^+ which dissociate, or (3*a–c*) intermediate 'resonant' excitation of doubly-excited (super-excited) 'Q' states, followed by autoionization into dissociative excited states of H_2^+ or dissociation into excited fragments:

$$\gamma + H_2 \rightarrow H_2^* \rightarrow H(1) + H(n) \qquad (14.7\ \text{eV}) \qquad (1)$$

$$\rightarrow H_2^{+*} + e^- \rightarrow H(n) + H^+ + e^- \qquad (\sim 36\ \text{eV}) \qquad (2)$$

$$\rightarrow H_2^{**} \rightarrow H_2^{+*} + e^- \rightarrow H(n) + H^+ + e^- \qquad (\sim 31\ \text{eV}) \qquad (3a)$$

$$\rightarrow H(n) + H^+ + e^- \qquad (\sim 31\ \text{eV}) \qquad (3b)$$

$$\rightarrow H(n) + H(n') \qquad (\sim 25\ \text{eV}) \qquad (3c)$$

where the energies in parentheses are the threshold values for the respective channels. For incident photon energies below 35 eV, the Q-state channels are the predominant mechanism for the production of excited photofragments. Above 40 eV, most fluorescence results from direct production of excited H_2^+ [4–8].

Dissociation of H_2 by VUV light is the most fundamental photochemical reaction. It plays an important role in the dynamics of the interstellar medium, atmospheres and plasmas [9–11]. While simple in concept, its theoretical description is difficult, owing in large part to the competing intermediate channels involved, the interplay between autoionization and

direct dissociation into neutral excited photofragments, and the multiple degeneracies of the asymptotic atomic energy levels [12, 13]. Thus, while heuristic fits of Franck–Condon excitation profiles to previous excitation function data have been good [7], *ab initio* calculations of the same data have not been available until recently [4]. Moreover, the assumptions necessary to produce good fits to the data are inconsistent with these theoretical predictions. The situation is exacerbated by the fact that different experimental data sets are in poor agreement [4].

In an attempt to resolve some of these issues, we have measured the excitation functions for Lyα and Hα light emitted from either excited H or D atoms following the photodissociation of H_2, HD and D_2. We have paid particular attention to the various systematic effects which affect these measurements. All available experimental data sets are compared to current theoretical calculations for Lyα and Hα production [4].

2. Experiment and systematics

These experiments were performed on the atomic, molecular and optical physics beam line (10.0.1.2) of the ALS at the Lawrence Berkeley National Laboratory (LBNL) in much the same way as previously described [4]. The beam line used a grazing-incidence spherical-grating monochromator (SGM) containing a grating with 380 lines mm^{-1}. The photon energy was scanned from 22 to 64 eV with a constant resolution of 40 meV and a constant step size of 400 meV. This was achieved by adjusting the entrance and exit slits of the monochromator at each energy to obtain the desired resolution. The incident photon flux was produced by an undulator and had a linear polarization of greater than 99% in the horizontal plane. This flux was monitored by a NIST-calibrated photodiode (IRD SXUV100).

In the experimental setup shown schematically in figure 1, the incident linearly-polarized photon flux was collimated to a beam approximately 1 mm in diameter which intersected a gas cell containing H_2, HD or D_2. The stainless steel cell was 30 cm in diameter and 29 cm tall and was flooded with a gas and directly pumped. This continuously flowing system provided stable pressures over the course of many hours. Two optical detection systems were used to collect light. Both were placed at the magic angle of 54.7° with respect to the incident flux polarization axis. Thus, the signal measured at each detector was proportional to the cross section and no polarization correction was required. The Hα detector had an optical train with a solid angle acceptance of 0.052 sr consisting of a GaAs photocathode photomultiplier tube (Hamamatsu R943-02) and an interference filter with a center-wavelength of 656.38 ± 0.46 nm (Andover 010FC12-50/6562). The Lyα detector with a solid angle of 0.078 sr comprised a channel-electron photomultiplier (PerkinElmer C1911P) with an integrated MgF_2 window which limited the detector's sensitivity to photons with wavelengths between 115 and 200 nm. Both detectors viewed an ∼1 cm section of the photon beam.

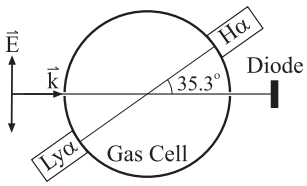

Figure 1. Schematic top view of apparatus. The electric field of the incident photon beam is in the plane of the Lyα and Hα detectors. The incident photon beam is collimated upstream of the gas cell and monitored downstream from the gas cell by a photodiode (see the text). Both Lyα and Hα detectors are positioned at the 54.7° magic angle with respect to the photon beam polarization axis.

The base pressure of the gas cell was 1.0×10^{-7} Torr. At this pressure, the observed background signal from the Lyα detector was due to the production of excited atomic N from photodissociation of N_2 [14]. The Hα background was approximately flat over the energy range of interest. These backgrounds were subtracted from their respective signals. The fluorescent signals from the Lyα and Hα channels were normalized to the photodiode (IRD SXUV100) current.

The uniform target gas pressure in the cell was kept at or below 10^{-4} Torr to minimize the effects of quenching collisions with H(2s) atoms [4, 15, 16]:

$$H_2 + H(2s) \rightarrow H_2 + H(2p) \rightarrow H_2 + H(1) + \gamma(122\ \text{nm}). \quad (4)$$

Since the H(2s) production cross section might have a different energy dependence than that of the Lyα excitation functions we wish to measure, it is important to ensure that this process does not affect our data. An estimate of the Lyα flux due to quenching can be made from the quenching probability (σnl) for a given target density n and interaction length l. Using the collisional quenching cross section σ for the H(2s) [15, 16] and the radius of the chamber, 15 cm, as the maximum possible path length, we find the quenching probability to be 10^{-3} for 10^{-5} Torr of H_2. To confirm that quenching was negligible, we measured the Lyα excitation function with H_2 cell pressures ranging from 10^{-4} to 10^{-6} Torr and observed no changes in its shape. We also did Monte Carlo simulations of process (4) in our experiment that showed quenching to be negligible. Indeed, the reason we replaced the effusive H_2 jet used in earlier work with a static gas cell was to improve the reliability of our Monte Carlo simulations. All of these results are consistent with earlier measurements discussed in [4] in which no shape change in the Lyα excitation function was observed for estimated effusive target densities between 10^{-2} and 10^{-5} Torr.

Although the incident VUV light was produced by an undulator and passed through a monochromator, it contained higher order components. In our experiment, baffles were used downstream of the exit slit of the SGM to suppress off-axis even harmonics. On-axis odd orders were suppressed by Al foil filters from the Lebow Company. Several runs were made with a 0.1 μm filter; most were made with a composite filter comprising a 0.1 μm and 0.15 μm foil stacked together. The transmission curves for the 0.1 and 0.25 μm composite

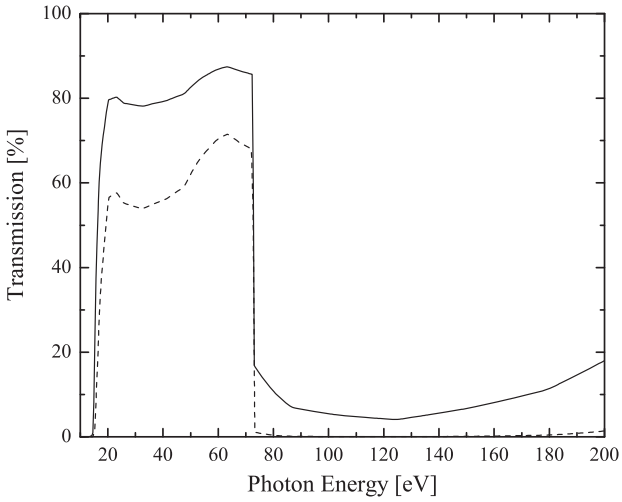

Figure 2. Transmission curve for 0.1 (solid line) and 0.25 μm (dashed line) thick aluminium foil filters [17].

filters, obtained from the CXRO group at Lawrence Berkeley Lab [17] are shown in figure 2. We found no significant differences between the excitation functions measured with the 0.1 and 0.25 μm filters, even though the thinner filter is roughly ten times more transparent to photons with energies just above the 72 eV Al cutoff. This gives us confidence that these filters removed the effects of higher odd harmonics in the beam.

Normalization to incident photon flux was accomplished by using a SXUV100 photodiode from IRD [18]. After 20 h of exposure or an integrated flux of approximately 7×10^{17} photons, the energy dependence of the diode response began to change. When the diode was removed from the system after more than 20 h of operation, the surface of the photodiode which the beam intersected was visibly discoloured. Although the target chamber was evacuated by a turbomolecular pump (Leybold TMP-150) backed by a Varian dry scroll pump resulting in a base pressure of 1×10^{-7} Torr without baking, the source of the blackened region appeared to be residual hydrocarbons in the vacuum which were deposited on the diode surface after cracking by the incident photon flux or the secondary electrons they produce [19, 20]. Measurements of diode surfaces taken after exposure under similar conditions show approximately 3 nm of carbon deposition [21]. Another possible cause of diode response variation is the radiation damage due to the high photon flux. The literature from IRD indicates that an integrated flux of 10^{19} photons at 50 eV will reduce the diode response to 90% of normal [18]. The variations in the diode response began occurring for at least an order of magnitude lower integrated flux. Thus, we believe that carbon contamination is the predominant cause of response decay.

Given the time dependence of the photodiode response (either the overall sensitivity or the energy dependence of this sensitivity), we took various measurements to determine how the measured excitation functions changed as the integrated flux increased. These measurements were taken at two different times, in December 2008 and June 2009. Between these two runs, the ALS upgraded from 'decay mode' (in which the ring is filled every 8 h) to 'top-off mode' (in which the ring is filled semi-continuously). It was found that during 'decay mode' runs the diode could be operated for approximately 20 h, corresponding to $\sim 7 \times 10^{17}$ photons, before the change in the response of the photodiode became the primary systematic error. In 'top-off mode', we determined that the integrated flux required to degrade the diode response was about the same but this flux now required only about 10 h to accumulate. Ultimately, we chose to mitigate this problem by using multiple 'fresh' spots on the 10×10 mm^2 active region of the SXUV100 diode. Using this precaution, the cross-section measurements of the June 2009 run agreed with those taken in December 2008.

Operating within these constraints, we measured the production of Lyα and Hα from the photodissociation of H_2, HD and D_2 from 22 to 64 eV. Multiple excitation functions were taken for each gas. Each data set underwent background subtraction and normalization to photodiode current which was corrected for the NIST calibrated efficiency. They were then combined using individual multiplicative scaling factors that minimized the energy-summed squared deviations of these scaled functions about their mean. The reported uncertainties at each energy are the standard deviation of the mean of the individual excitation functions about their mean. Since our measurements are not absolute, we have scaled our results to the theoretical results of Bozek *et al* [4] at 50 eV. This produces the best agreement between current experimental results and the available theory. Using the Lyα count rate at 35 eV for H_2 of 10 kHz, an efficiency of the Lyα detector of 10%, a photon flux of 10^{15} photons per second, an interaction length of 1 cm (as viewed by the detector), and a pressure of 10^{-6} Torr at room temperature, we estimate the absolute cross section for the production of Lyα from H_2 photodissociation to be $\sim$0.1 Mbarn, which is in (surprisingly) good agreement with theory [4].

3. Data and discussion

Figures 3–8 contain our current results compared to both theory and previous experimental results [1–4, 8, 22, 23, 25, 26]. The theoretical curves presented in these figures are based on state-of-the-art calculations from Bozek *et al* [4], and are discussed in detail in that reference and references therein. They represent solutions of the time-dependent Schrödinger equation using the exact non-relativistic Hamiltonian of H_2 and the radiation–molecule interaction potential in the dipole approximation and the velocity gauge. Since our experimental results are not absolute, we have chosen to normalize our data (both of Bozek *et al* [4] and our current results) to theory at 50 eV. In this portion of the spectrum, the shape of our Lyα relative cross section closely matches that of theory. Normalization of the Hα relative cross section at 50 eV was done for consistency. The systematic differences between the older data of Bozek *et al* [4] (blue circles) and the present data (red squares) shown in figures 3, 5, 6 and 8 illustrate the effects of high harmonic components of the beam and temporal degradation of the photodiode, as discussed above.

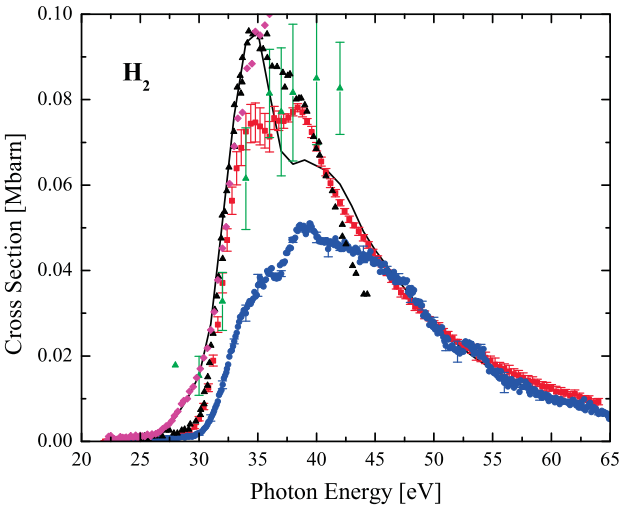

Figure 3. Excitation functions for Lyα photoemission resulting from H_2 photodissociation by linearly-polarized light. Red squares represent experimental results normalized to theory at 50 eV; blue circles results of Bozek *et al* normalized at 50 eV [4]; green/grey triangles absolute results of Glass-Maujean *et al* [1]; black triangles results of Odagiri *et al* [3]; magenta diamonds results of Arai *et al* [23]; and the solid line represents the theoretical result from Bozek *et al* [4].

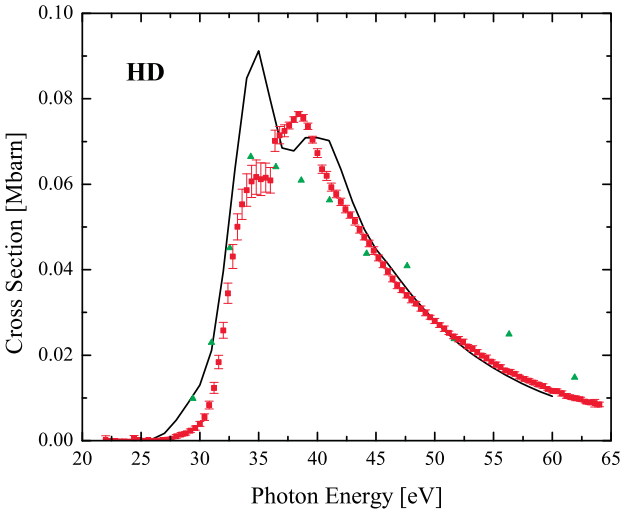

Figure 4. The same as figure 3 but for HD molecules. Green triangles represent the absolute results of Glass-Maujean [8] and the solid line represents the theoretical result [26].

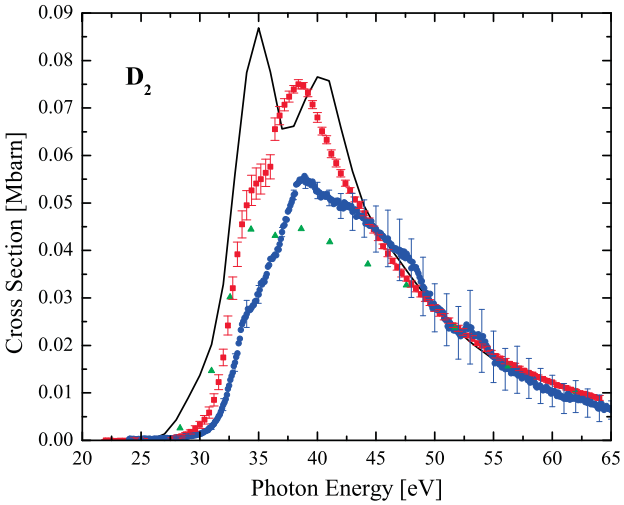

Figure 5. The same as figure 3 but for D_2 molecules. Green triangles represent absolute results of Glass-Maujean [8].

Below ~40 eV, the new data are consistently higher in all of the excitation functions. We did several tests to examine the effect of Al filters on the shape of the excitation functions for Lyα radiation. In experiments done with 'fresh' photodiodes, removal of the high harmonic component of the incident photon beam with these filters increased the excitation function peak heights by roughly 15% relative to the value at 50 eV. This alone is not sufficient to explain the difference we observe between the two data sets. We attribute the major source of difference to changes in the response of the photodiode that occurred because of carbon contamination. This consisted both of changes in the overall sensitivity and changes in the energy response of the photodiode.

We now consider the effect on the excitation functions of the isotopic composition of the target, considering only the present data and the theory of Bozek *et al* [4] (see figures 3–8). The Lyα data are more sensitive to isotopic composition than the Hα data. The Lyα excitation functions are characterized by two local maxima, nominally at energies of 35 and 39 eV. (In the D_2 experimental data, the lower energy feature is a 'shoulder'.) The low-energy feature is primarily due to dissociation of Q_2 states (processes (3)), while the high-energy peak is the result of non-resonant H_2 ionization and dissociation (process (2)) [4]. In both theory and experiment, the cross section associated with the low-energy feature exhibits a significant drop as the target mass is increased. This is consistent with this feature being due to processes (3); as the mass increases the Q_2 state dissociates more slowly and autoionization (process (3*a*)) diverts an increasing amount of flux away from neutral–neutral production (process (3*c*)). However, theory predicts an increase in the cross section of the high-energy Lyα peak with increasing mass, while we measure a level or downward trend.

In the case of the Hα excitation functions, two well-defined local maxima are observed at about 37 and 48 eV, again corresponding to Q_2 dissociation and non-resonant dissociative ionization, respectively [4]. Compared with the Lyα data, the peak cross sections are relatively insensitive to the target mass. The low-energy peak does, however, increase slightly with increasing mass in both experiment and theory. This is inconsistent with the idea discussed above that autoionization should lower the fluorescence cross section of the low-energy peak as the target mass increases, suggesting that channel (3*a*) may dominate the dissociation process leading to Hα for all three targets. There is a hint of some target-mass-dependent substructure in the low-energy peak. While the D_2 maximum is quite symmetric about its peak at 37 eV, the equivalent HD peak has a weak 'shoulder' at ~35 eV, and the H_2 peak is somewhat asymmetric about its maximum between 35 and 38 eV.

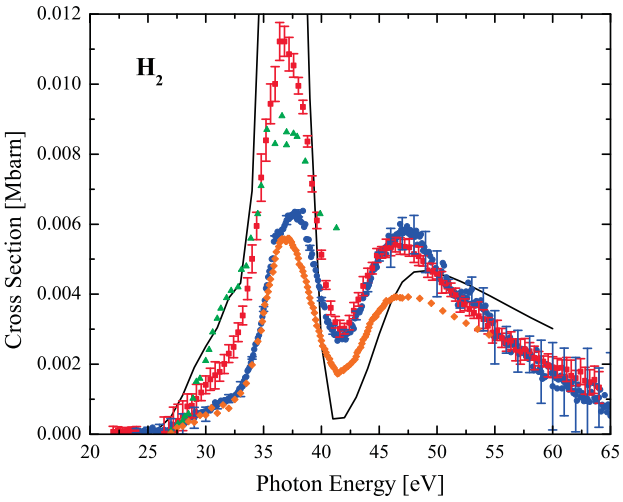

Figure 6. Excitation functions for Hα photoemission resulting from H_2 photodissociation by linearly-polarized light. Experiment: red squares represent results normalized to theory at 50 eV; blue circles the experimental result from Bozek *et al* also normalized at 50 eV [4]; green triangles the absolute results of Glass-Maujean *et al* [25]; orange diamonds the absolute results of Melero García *et al* [2]; and the solid line represents the theoretical result from Bozek *et al* [4] which peaks at 37 eV with a value of 0.0295 Mbarn.

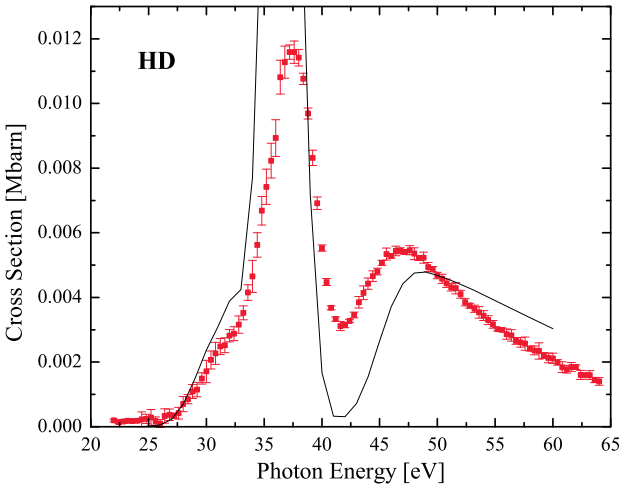

Figure 7. The same as figure 6 but for HD molecules. The theoretical result peaks at 36 eV with a value of 0.0304 Mbarn from [26].

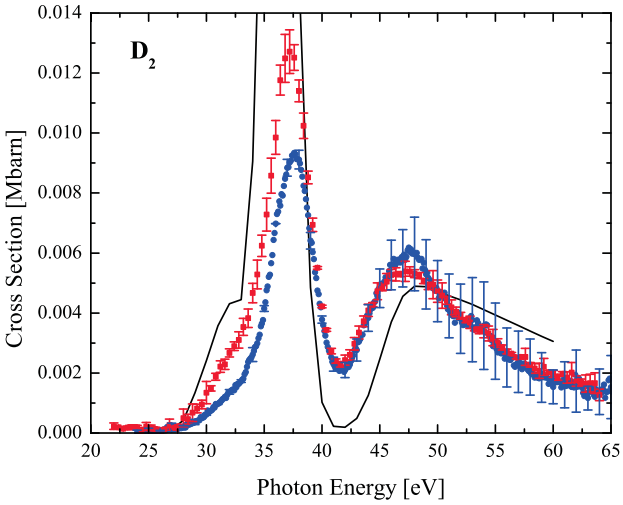

Figure 8. The same as figure 6 but for D_2 molecules. The theoretical result peaks at 36 eV with a value of 0.0340 Mbarn from [4].

Our results are susceptible to the effects of cascading and *l*-dependent detection efficiency [2, 4], which have been discussed in detail by Glass-Maujean and co-workers [2, 25] and by Bozek *et al* [4]. The latter effects are not relevant for Lyα fluorescence, and are non-negligible only for emission from the 3s state in the energy regions below 33 eV and above 42 eV. For Lyα excitation functions in the photon-energy region between 35 and 45 eV, cascading may account for as much as 30% of the observed fluorescence. We note, however, that since the theory and experimental results for the excitation cross sections above 50 eV are in good agreement (after normalization), subtraction of a cascading contribution at lower energy will only degrade the overall agreement between experiment and theory. Moreover, above 30 eV, cascade contributions have only weak energy dependence and thus have minimal effect on the shape of the Hα excitation functions (see [4], figure 7).

When considering the contributions of the various Q states and direct, non-resonant ionization to the total Lyα signal, it is interesting to compare the results of *ab initio* theory [4] and a heuristic fit to the data using the method of Glass-Maujean and co-workers. In the latter case, we used absorption profiles obtained by Glass-Maujean and Schmoranzer [7], which in turn were based on the potential energy curves of Sanchez and Martin [27] and Sharp [28] and the electronic transition dipole moment functions calculated by Borges and Bielschowsky [13]. Figure 9 shows the results of this fitting procedure; table 1 shows the relative contributions of the various Q states and non-resonant ionization. It should be noted that this fit is not unique and other combinations of states may yield fits of similar quality. Attempts to include several Q $^1\Sigma$ states, however, produced qualitatively worse results. Each absorption profile was normalized to unity at its maximum.

Table 1. Contributions of various Q states to the measured H_2 Lyα excitation function as determined by empirical fitting (see the text, figure 9).

State	Contribution (Mbarn)	Assignment	Fragments
$Q_1\ ^1\Pi(1)$	0.008	$^1\Pi_u(2p\sigma_u 3d\pi_g)$	H(1s) + H(2p)
$Q_2\ ^1\Pi(1)$	0.060	$^1\Pi_u(2p\pi_u 2s\sigma_g)$	H(2p) + H(2s)
$Q_2\ ^1\Pi(4)$	0.051	$^1\Pi_u(2p\pi_u 4s\sigma_g)$	H(2p) + H(n = 4)
$Q_3\ ^1\Pi(2)$	0.013	$^1\Pi_u(2s\sigma_g 3p\pi_u)$	H(2s) + H($3l$)
H_2^+	0.054	$2p\pi_u$	H(n = 2p) + H^+

Thus, the contributions to the fit in table 1 represent the maximum absolute cross section (Mb) for each of the fitted profiles. Our fit reproduces the data quite well below 45 eV, indicating the importance of both the doubly-excited Q states and non-resonant ionization.

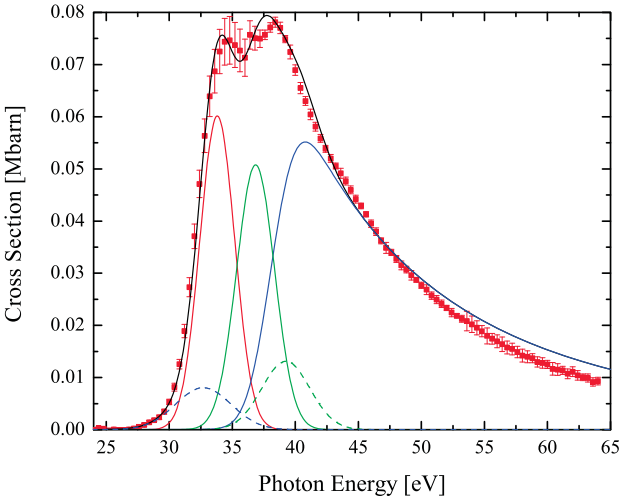

Figure 9. Red squares represent experimental results from figure 3. Heuristic fit contributions: solid green line represents $Q_2\ ^1\Pi(4)$; solid blue line H_2^+ non-resonant direct ionization; solid red line $Q_2\ ^1\Pi(1)$; dashed green line $Q_3\ ^1\Pi(2)$; dashed blue line $Q_1\ ^1\Pi(1)$; and solid line the total.

The most interesting result of the fit shown in figure 9 is the need for a significant contribution from a Q_3 state which, according to the theory of Bozek *et al* [4], has essentially no probability of being excited. The presence of a Q_3 contribution is consistent with the conclusions of [7], even though the present data differ significantly in other ways. Our fit also gives more weight to non-resonant ionization in comparison with Q_2 than does the theory. It is clear from the observed 27 eV threshold energy of the excitation function that $Q_1\ ^1\Sigma(1)$ states do not contribute to the Lyα fluorescence. This is consistent with previous measurements [3, 25]. Such a component might be expected given its predicted excitation threshold at ~25 eV [7]. However, the $Q_1\ ^1\Sigma(1)$ states are expected to result in little fluorescence because of their propensity to produce ion pairs [25].

Because of their comprehensive nature, the present measurements provide a stringent test of theory. They do, however, represent an integration over all possible photofragmentation channels leading to a given separated-atom *n*-level. As such, it is difficult to isolate individual dissociation processes. The detailed interaction between the various dissociation channels is very difficult to characterize theoretically in H_2. This is because the asymptotic degeneracy of the separated atom states causes large interactions between the converging adiabats at intermediate nuclear separations. This difficulty is likely a significant contributor to the disagreements we observe between the experiment and theory. One way to further probe the difference between the theoretical and experimental results is to perform state-specific measurements which would allow a more detailed examination of some of the processes involved in the dissociation. Such state-specific measurements of the dissociation of doubly-excited H_2 into H(2p) + H(2p) using coincident detection of Lyα photons have been done [3, 24]. However these are difficult measurements and necessarily limited in the choice of final states. To our knowledge, no theoretical calculations have been done to compare with these measurements.

It may also be possible to further test elements of theory by measuring the linear and circular polarization of the fluorescence of photofragments created by the dissociation of states excited by linearly- or circularly-polarized light. Such polarization measurements contain information about coherences between dissociating channels and thus provide a different way to probe the complex interaction between the various dissociation channels.

4. Conclusion

The comprehensive excitation-function data set for Lyα and Hα fluorescence from the photodissociation of H_2 and D_2 for energies at which doubly-excited states are produced has been extended to include HD targets. Previous measurements of this process by us were hampered by systematic effects which have been corrected. However, agreement between the existing experimental measurements and the best available theory is still poor. Extensive development of theoretical calculations in conjunction with more detailed experimental measurements to elucidate the causes of these discrepancies is highly desirable.

Acknowledgments

We would like to thank the referees for many helpful comments, J F Perez-Torres and Drs Fernando Martin and Jose Luis Sanz-Vicario for extending their theory to HD and Drs Harvey Gould and Jack Maseberg for useful conversations. This work was funded by the DOE through the use of the ALS, the NSF through grants PHY-0653379 and PHY-0821385, and ANSTO (Access to Major Research Facilities Programme).

References

[1] Glass-Maujean M, Klumpp S, Werner L, Ehresmann A and Schmoranzer H 2004 *J. Phys. B: At. Mol. Opt. Phys.* **37** 2677
[2] Melero García E, Álvarez Ruiz J, Menmuir S, Rachlew E, Erman P, Kivimäki A, Glass-Maujean M, Richter R and Coreno M 2006 *J. Phys. B: At. Mol. Opt. Phys.* **39** 205
[3] Odagiri T, Murata M, Kato M and Kouchi N 2004 *J. Phys. B: At. Mol. Opt. Phys.* **37** 3909
[4] Bozek J D, Furst J E, Gay T J, Gould H, Kilcoyne A L D, Machacek J R, Martin F, McLaughlin K W and Sanz-Vicario J L 2006 *J. Phys. B: At. Mol. Opt. Phys.* **39** 4871
Bozek J D, Furst J E, Gay T J, Gould H, Kilcoyne A L D, Machacek J R, Martin F, McLaughlin K W and Sanz-Vicario J L 2008 *J. Phys. B: At. Mol. Opt. Phys.* **41** 039801
Bozek J D, Furst J E, Gay T J, Gould H, Kilcoyne A L D, Machacek J R, Martin F, McLaughlin K W and Sanz-Vicario J L 2009 *J. Phys. B: At. Mol. Opt. Phys.* **42** 029801
[5] Kouchi N, Ukai M and Hatano Y 1997 *J. Phys. B: At. Mol. Opt. Phys.* **30** 2319
[6] Hatano Y 1999 *Phys. Rep.* **313** 109
[7] Glass-Maujean M and Schmoranzer H 2005 *J. Phys. B: At. Mol. Opt. Phys.* **38** 1093
[8] Glass-Maujean M 1986 *J. Chem. Phys.* **85** 4830
[9] Ferland G J 2003 *Annu. Rev. Astron. Astrophys.* **41** 517

[10] Liang M-C, Parkinson C D, Lee A Y-T, Yung Y L and Seager S 2003 *Astrophys. J. Lett.* **596** L247
[11] Fantz U 2005 Atomic and molecular data and their applications *Proc. Joint Meeting of the 14th Int. Toki Conf. on Plasma Physics and Controlled Nuclear Fusion and the 4th Int. Conf. on Atomic and Molecular Data and Their Applications* ed T Kato, D Kato and H Funaba (*AIP Conf. Proc.* vol 771)
[12] Martin F 1999 *J. Phys. B: At. Mol. Opt. Phys.* **32** R197
[13] Borges I J and Bielschowsky C E 2000 *J. Phys. B: At. Mol. Opt. Phys.* **33** 1713
[14] Ukai M, Kameta K, Kouchi N and Hatano Y 1992 *Phys. Rev.* A **46** 7019
Erman P, Karawajczyk A, Rachlew-Kallne E, Sorensen S L, Stromholm C and Kirm M 1993 *J. Phys. B: At. Mol. Opt. Phys.* **26** 4483
[15] Weissmann H, Hartmann W and Burch D S 1987 *Z. Phys.* D **7** 119
[16] Fleming E, Wilhelmi O, Schmoranzer H and Glass-Maujean M 1995 *J. Chem. Phys.* **103** 4090
[17] http://www-cxro.lbl.gov/
[18] International Radiation Devices, Inc., www.ird-inc.com
[19] Rosenberg R A and Mancini D C 1990 *Nucl. Instrum. Methods Phys. Res.* A **291** 101–6
[20] Boller K, Haelbich R-P, Hogrefe H, Jark W and Kunz C 1983 *Nucl. Instrum. Methods* **208** 273
[21] Gullikson E 2008 Advanced Light Source, Lawrence Berkeley National Laboratory private communication
[22] Glass-Maujean M, Frohlich H and Martin P 1995 *Phys. Rev.* A **52** 4622
[23] Arai S, Yoshimi T, Morita M, Hironaka K, Yoshida T, Koizumi H, Shinsaka K, Hatano Y, Yagishita A and Ito K 1986 *Z. Phys.* D **4** 65
[24] Arai S, Kamosaki T, Ukai M, Shinsaka K and Hatano Y 1988 *J. Chem. Phys.* **88** 3016
[25] Glass-Maujean M 1988 *J. Chem. Phys.* **89** 2839
[26] Perez-Torres J F, Sanz-Vicario J L and Martin F 2008 private communication
[27] Sanchez I and Martin F 1997 *J. Chem. Phys.* **106** 7720
Sanchez I and Martin F 1999 *J. Chem. Phys.* **110** 6702
[28] Sharp T E 1970 *At. Data Nucl. Data Tables* **2** 119